RNA aptamers as pathway-specific MAP kinase inhibitors

Scott D Seiwert [1], Theresa Stines Nahreini [2], Stefan Aigner [1], Natalie G Ahn [2] and Olke C Uhlenbeck [1]

Background: In eukaryotic cells, many intracellular signaling pathways have closely related mitogen activated protein kinase (MAPK) paralogs as central components. Although MAPKs are therefore obvious targets to control the cellular responses resulting from the activation of these signaling pathways, the development of inhibitors which target specific cell signaling pathways involving MAPKs has proven difficult.

Results: We used an RNA combinatorial approach to isolate RNAs that inhibit the in vitro phosphorylation activity of extracellular regulated kinase 2 (ERK2). These inhibitors block phosphorylation by ERK1 and ERK2, but do not inhibit Jun N-terminal kinase or p38 MAPKs. Kinetic analysis indicates these inhibitors function at high picomolar concentrations through the steric exclusion of substrate and ATP binding. In one case, we identified a compact RNA structural domain responsible for inhibition.

Conclusions: RNA reagents can selectively recognize and inhibit MAPKs involved in a single signal transduction pathway. The methodology described here is readily generalizable, and can be used to develop inhibitors of MAPKs involved in other signal transduction pathways. Such reagents may be valuable tools to analyze and distinguish homologous effectors which regulate distinct signaling responses.

[1]Department of Chemistry and Biochemistry, University of Colorado at Boulder, Boulder, CO 80309-0215, USA
[2]Howard Hughes Medical Institute, University of Colorado at Boulder, Boulder, CO 80309-0215, USA

Correspondence: Scott Seiwert, Olke Uhlenbeck and Natalie Ahn
E-mail: scott.seiwert@colorado.edu
E-mail: olke.uhlenbeck@colorado.edu
E-mail: ahnn@spot.colorado.edu

Keywords: Inhibitor; Kinase; Kinetics; Mitogen activated protein kinase; RNA aptamer; RNA selection

Received: **19 May 2000**
Revisions requested: **29 August 2000**
Revisions received: **6 September 2000**
Accepted: **7 September 2000**

Published: **20 September 2000**

Chemistry & Biology 2000, **7**:833–843

1074-5521/00/$ – see front matter

PII: S1074-5521(00)00032-6

Introduction

Mitogen activated protein kinases (MAPKs) are terminal components of evolutionarily conserved protein-phosphorylation cascades utilized in a diverse array of eukaryotic signal transduction pathways. When activated, MAPKs phosphorylate transcription factors, cytoskeletal proteins, and other protein kinases and cellular components to promote pathway-specific changes in cell physiology [1]. In mammalian cells, different MAPKs are involved in specifying responses which include cell proliferation, apoptosis, and differentiation [1]. Inappropriate activation of specific MAPK pathways is associated with various disease states in humans, including cancer [2] and autoimmune diseases [3]. Although events which lead to extracellular regulated kinase 1/2 (ERK1/2) activation are understood, the molecular targets of ERK1/2 which promote proliferative responses are much less well defined, reflecting a general problem in analyzing the changes in gene expression promoted by signal transduction pathways. Clearly, techniques providing a rapid and accessible means to develop inhibitors that block specific signal transduction pathways would be valuable to address this issue.

Despite their potential importance, the development of inhibitors that target specific MAPK pathways has been difficult due to the large number of highly related MAPK variants. Mammalian cells contain at least 12 MAPK paralogs that comprise at least five sequence subfamilies [4]. At least three of these are associated with distinct signaling pathways; the ERK1/2 and ERK5 subfamilies mediate growth factor signaling, while the c-JUN N-terminal kinase/stress activated protein kinase (JNK/SAPK) and the p38 MAPK subfamilies are implicated in cell stress and inflammatory responses. Two additional proteins (ERK3a and ERK3b) comprise a sequence subfamily that functions in signaling pathways not currently defined.

Most of the small molecule inhibitors of protein kinases produced thus far act as competitive inhibitors of ATP binding [5–8]. Such inhibitors must derive their specificity from the structural features of the evolutionarily conserved ATP binding pocket which are unique to their particular kinase target. Consequently, it has proven difficult to produce small molecule inhibitors that can effectively discrim-

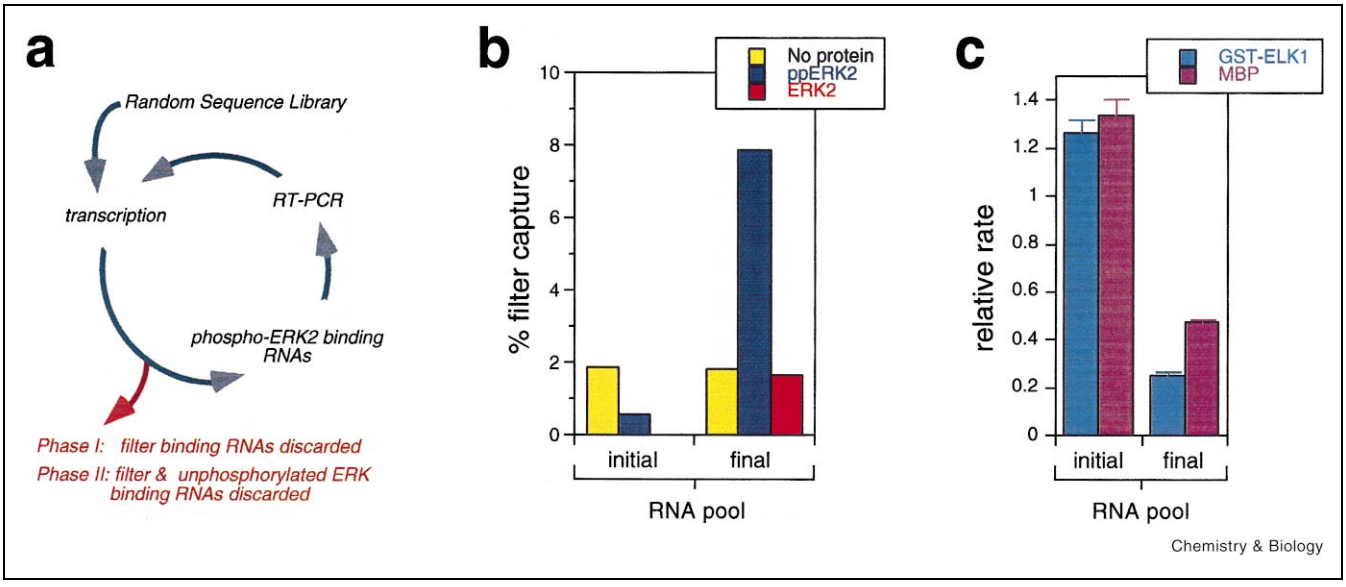

Figure 1. Iterative RNA selection. **(a)** Iterative selection methodology. The initial RNA pool contained $\sim 2 \times 10^{14}$ members. During the first phase of iterative selection, the ppERK2 concentration was progressively reduced from 250 nM to 100 nM. In the second phase, the pool RNA was incubated with unphosphorylated protein and nitrocellulose membrane capture was used to remove molecules that associated with the unphosphorylated form of ERK2. After several steps of membrane capture in the presence of ERK2, the remainder of the RNA pool was incubated with ppERK2 and RNAs capable of associating with ppERK2 were isolated, again by nitrocellulose membrane capture. **(b)** RNA pool binding to phosphorylated and unphosphorylated ERK2. Percent of the initial and final RNA pool that associated with 1 nM ppERK2 (blue) or 1 nM ERK2 (red) was assayed by capture of RNA–protein complexes on nitrocellulose membranes. % RNA pool captured in the absence of protein is indicated (yellow). **(c)** RNA pool inhibition of ppERK2 catalyzed phosphorylation. In vitro phosphorylation of 1.25 μM GST-ELK1 (blue) or 0.25 mg/ml MBP (purple) catalyzed by 10 nM ppERK2 contained 20 nM of the initial or final RNA pool, or no RNA. Data are expressed as the average relative rate ($k_{rel} = k_{RNA}/k_{no\ RNA}$) from two or more experiments and the standard deviation between experiments is indicated. The lower extent of inhibition seen with the MBP substrate most likely reflects its ability to sequester RNA through nonspecific electrostatic interactions due to its high p*I* (p*I* = 11). Therefore, the GST-ELK1 fusion protein was used as substrate in all future experiments.

inate between the estimated 2500 protein kinases present in mammalian cells. For example, the specificity of pyridinylimidazole compounds for p38α/β MAPKs depends largely on the side chain size of a single amino acid in the ATP binding pocket [9]. Any protein kinase that contains an amino acid side chain of equivalent or smaller size at the corresponding position (such as type II transforming growth factor β receptor) are somewhat sensitive to these compounds [10]. Thus, the development of more specific protein kinase inhibitors that target other structural elements in protein kinases could in principle provide greater specificity of inhibition. Ideally, these inhibitors would recognize a complex, functionally important epitope unique to all of the MAPK subfamily members involved in a single cell signaling pathway.

In MAPKs, the 'activation lip' represents such a target. The activation lip is found at the interface of the N- and C-terminal folding domains and contains conserved threonine and tyrosine residues whose phosphorylation activates the kinase. Dual phosphorylation activates the kinase by reorienting the two domains to align active site residues for catalysis [11]. Thus, the activation lip is a crucial component of MAPK function. Because the activation lip differs in sequence between the various MAPK subfamilies involved in different signal transduction pathways [4], it therefore represents a potentially useful target for pathway-specific inhibitors.

Here, we describe the development of novel MAPK inhibitors targeted to the activation lip of ERK2. Our strategy relied on an RNA combinatorial approach which allows RNA molecules that perform a desired function to be isolated from a large ($\sim 10^{14}$–10^{15}) collection of random sequence RNA through iterative enrichment [12]. This methodology has been previously exploited to identify high affinity RNA ligands (RNA aptamers) to small molecules and proteins. RNA aptamers that bind to enzymes such as proteases [13], protein phosphatases [14], and protein kinases [15] can inhibit the function of their target in vitro, making RNA iterative selection a useful means to develop inhibitors of protein function. Since such RNA aptamers can be expressed from cassettes in cultured cells [16,17] and can function as inhibitors in vivo [18–20], this

approach represents a potentially valuable means to dissect cellular processes.

Results

RNA selection

In order to identify RNAs that recognize activated ERK2, a library of DNA molecules containing 134 randomized positions was constructed [21] and transcribed for use in the initial round of an iterative selection scheme that had two phases (Figure 1a). In the first phase of selection, RNA molecules that bound to high (100 nM) concentrations of the diphosphorylated form of ERK2 (ppERK2) were enriched from the initial, random RNA pool. The second phase of selection included a negative selection step in order to remove RNAs that bound to the unphosphorylated form of ERK2, with the intent of isolating only those RNAs that bound epitopes not shared by both forms of the protein. Iterative selection was terminated when a significant fraction of the RNA pool bound to 1 nM ppERK2, but showed no binding to non-phosphorylated ERK2 at the same concentration (Figure 1b).

To determine whether the final ppERK2 binding RNA pool contained molecules that could inhibit the kinase activity of ppERK2, the RNA pool was assayed for the ability to inhibit ppERK2 catalyzed phosphorylation in vitro (Figure 1c). Phosphorylation of a GST-ELK1 fusion protein catalyzed by 10 nM ppERK in the presence of 20 nM of the final pool RNA displayed a relative rate of approximately 25% that observed in its absence. Similarly, phosphorylation of myelin basic protein (MBP) by ppERK2 displayed a relative rate of 53%. Importantly, the initial, random sequence pool of RNA did not diminish the rate of ppERK2 catalyzed phosphorylation of either protein under identical conditions (Figure 1c). Thus, our selection protocol was successful in enriching for RNA molecules that inhibit phosphorylation catalyzed by ppERK2.

To identify the most potent inhibitors in the final pool of RNA, individual RNAs comprising this pool were cloned and assayed individually for their ability to inhibit ppERK2 catalyzed phosphorylation of MBP. Four of the 20 RNAs screened were found to inhibit this reaction to an extent greater than that displayed by the final RNA pool (data not shown). Based on their sequences, these highly inhibitory RNAs comprise two classes. Family I consisted of three related members, while family II contained a single member. Since the initial RNA library sampled only $\sim 4.2 \times 10^{-65}\%$ of all possible random sequences, it is extremely unlikely that all three members of family I were present in the initial RNA pool and therefore must have arisen through PCR mutagenesis during the iterative selection procedure.

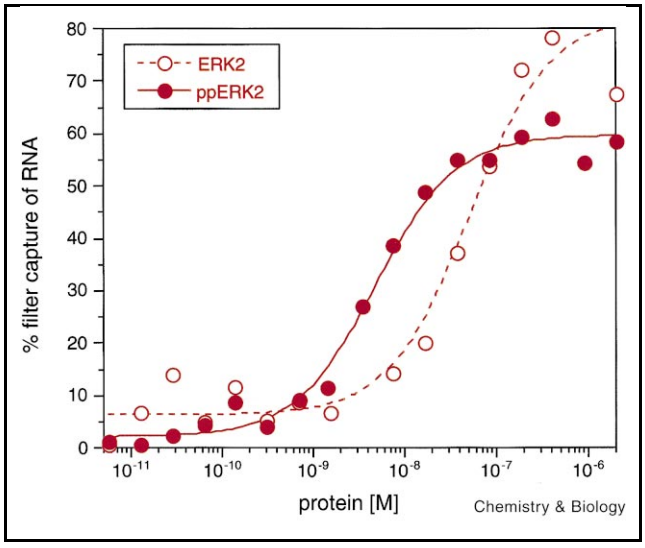

Figure 2. Dissociation constants of family II RNA. Trace, 5′-end labeled family II RNA was incubated with diphosphorylated or unphosphorylated ERK2 over a protein concentration range from 2 μM to 5.6 pM. RNA–protein complexes were captured on nitrocellulose membranes and data were analyzed as described [31].

We examined the dissociation constants for both the unphosphorylated and diphosphorylated forms of ERK2 of the family II RNA and the most potent family I RNA (Figure 2 and data not shown). Family II RNA has a K_d for ppERK2 of 4.7 nM whereas the K_d is approximately 10-fold higher for the unphosphorylated form of ERK2 (50 nM) (Figure 2). In contrast, family I RNA binds with roughly the same affinity to both phosphorylated and unphosphorylated forms of ERK2 ($K_d = 1.3$ nM ppERK2, $K_d = 2.3$ nM ERK2). The difference in affinity between phosphorylated and unphosphorylated protein observed

Table 1
Kinetic analysis of RNA inhibitors[a].

RNA family	Substrate examined	Inhibition type	K_i (nM)
I	GST-ELK1	competitive	0.3
II	GST-ELK1	competitive	5.1
II	ATP[b]	competitive	16.1

[a]See Figure 3 and Materials and methods for experimental details.
[b]ATP concentration varied from 100 μM to 6.25 μM.

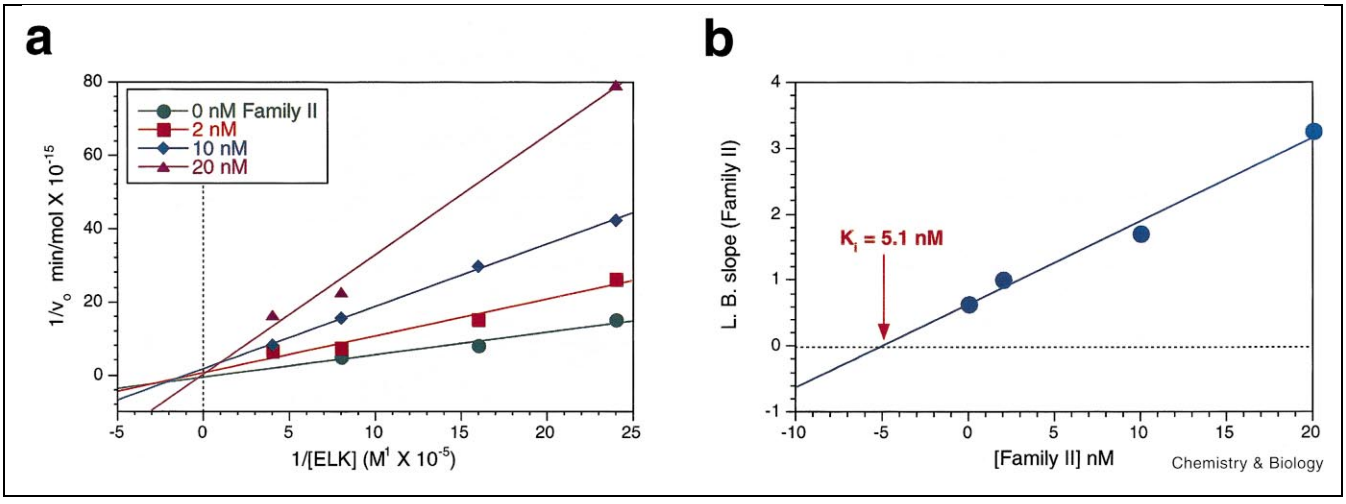

Figure 3. Representative kinetic analysis of RNA inhibitors. **(a)** Lineweaver–Burk analysis of the effects of family I RNA. Initial rates of ppERK2 catalyzed phosphorylation of GST-ELK1 were determined at substrate concentrations ranging from 1.25 μM to 160 nM, in the presence of 0, 2, 5, or 20 nM family II RNA. ppERK2 was present at 0.5 nM. **(b)** Family I K_i determination. Line slopes for data in panel **a** were calculated by linear regression and plotted relative to the concentration of inhibitor that generated the line slope; the *X*-intercept gives $-K_i$.

with the family II RNA indicates that it derives part of its binding energy from epitopes specific to the phosphorylated protein.

Kinetic characterization

Kinetic analysis was used to assess the nature of the inhibition promoted by the most potent family I and family II RNA. For each RNA family, K_m and V_{max} values for ppERK2 catalyzed phosphorylation of GST-ELK1 were determined at saturating concentrations of ATP. Parallel kinetic experiments were performed in the presence of several different inhibitor concentrations. Lineweaver–Burk analysis of these data indicates that both RNA families function as competitive inhibitors of substrate binding since both affect the K_m for the GST-ELK1 substrate (Figure 3a, Table 1). Thus, both inhibitors block association of the protein substrate with ppERK2. K_i values for both RNA families were obtained by plotting the line slopes of the Lineweaver–Burk data relative to the inhibitor concentration (Figure 3b, Table 1). The most potent family I inhibitor has a K_i of approximately 0.3 nM, while the family II RNA displays a K_i of approximately 5.1 nM. As expected, these values are similar to the dissociation constants determined for family I and family II RNAs for ppERK2 (1.3 nM and 4.7 nM, respectively). These values also compare favorably with those displayed by small molecule inhibitors of protein kinases. For example, the pyridinylimidazole compound 4-(fluorophenyl)-2-(4-methylsulfinylphenyl)-5-(4-pyridyl)-imidazole (SB203580) displays a K_i between 21 nM [6] and 34 nM [22] for p38.

Small molecule inhibitors of p38α/β, and of other protein kinases generally, act by preventing the association of ATP with their kinase target [5]. Therefore, we examined whether the family II RNA aptamer also functioned as a competitive inhibitor of ATP association with ppERK2. Again, K_m and V_{max} values were measured at various concentrations of inhibitor, but in this case GST-ELK1 was held at a high concentration as the concentration of ATP was varied. Lineweaver–Burk analysis of these data demonstrate that the family II RNA also behaves as a competitive inhibitor of ATP binding (Table 1). However, the apparent K_i ATP (16.1 nM) is approximately three times greater than the K_i for GST-ELK1 (5.1 nM, Table 1).

This kinetic analysis suggests that our iterative RNA selection protocol isolated an RNA inhibitor (family II) that acts by preventing the binding of both substrate and ATP to ppERK2, most likely through steric exclusion. Thus, the RNA inhibitors that we report have a novel mechanism of action relative to small molecule protein kinase inhibitors; they increase the K_m for the substrate as well as prevent the ATP phosphoryl donor from interacting with ppERK2 (Figure 3, Table 1).

Inhibitor specificity

Human ERK1 (hERK1) is nearly identical in sequence to rat ERK2 (rERK2) (99.1% identity) and functions along with ERK2 in mediating growth factor signaling in mammalian cells [1]. To test whether either family of RNA inhibitor could affect the activity of hERK1, family I and

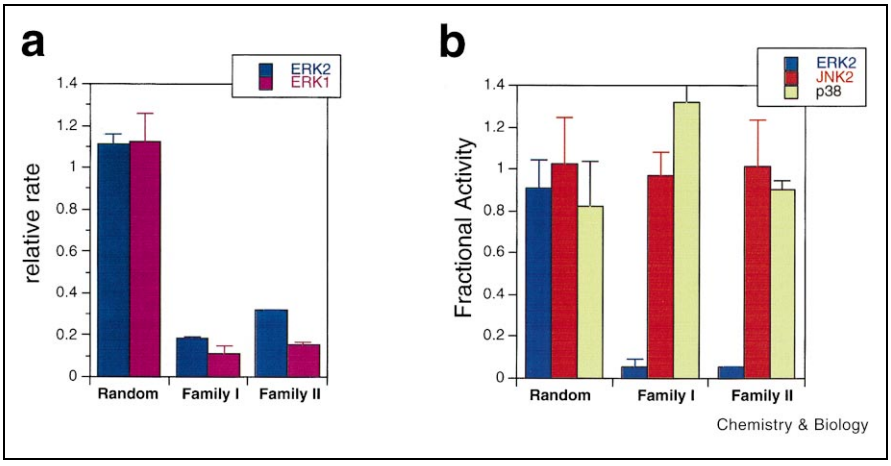

Figure 4. RNA inhibitors are specific for ERK1/2 MAPKs. All data are derived from two or more measurements, but in some cases errors are too small be visualized. **(a)** ERK1/2 catalyzed phosphorylation. In vitro phosphorylation of 1.25 μM GST-ELK1 catalyzed by 10 nM activated ERK2 (blue) or 10 nM activated ERK1 (purple), including 12 nM family I RNA, 12 nM family II RNA, 12 nM initial RNA pool, or no RNA. Data are expressed as average relative rates ($k_{rel} = k_{RNA}/k_{no\ RNA}$) from two or more experiments. **(b)** Phosphorylation catalyzed by ERK2, JNK, and p38. In vitro phosphorylation of 1.25 μM GST-ELK1 catalyzed by 0.1 μM activated ERK2 (blue), 0.1 μM activated JNK2 (orange), or 0.1 μM activated p38 (yellow) in the presence of 0.12 μM family I RNA, 0.12 μM family II RNA, 0.12 μM of the initial RNA pool, or without RNA present. Extent of reaction is expressed as the average fraction of the phosphorylation activity observed in the absence of RNA seen in two or more experiments.

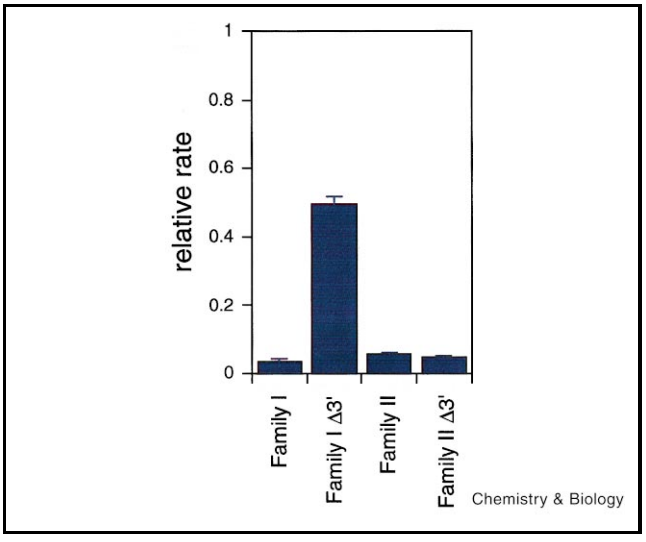

Figure 5. Localization of family I and family II inhibitory domains. Phosphorylation of 1.25 μM GST-ELK1 catalyzed by 10 nM ERK2 included full length family I or full length family II RNAs (189 nucleotides), or 3′ truncated versions of each containing the 5′-most 101 nucleotides (family I Δ3′ and family II Δ3′, respectively) at 20 nM. Data are expressed as average relative rates, $k_{rel} = k_{RNA}/k_{no\ RNA}$ from two experiments.

family II RNAs were assayed for their ability to inhibit hERK1 catalyzed phosphorylation of the GST-ELK1 fusion protein (Figure 4a). Both RNA families were equally effective in inhibiting the phosphorylation catalyzed by low (10 nM) concentrations of either hERK1 or rERK2 (Figure 4a). A pool of random sequence RNAs at this same concentration had no effect on phosphorylation catalyzed by hERK1 or by rERK2 (Figure 4a) as expected (Figure 1c). Thus, the modest difference in sequence between these two proteins does not affect the association and consequent functional inhibition by family I or family II RNAs.

To determine whether either of the ppERK1/2 inhibitors displayed inhibitory activity for members of the JNK/SAPK or the p38 subfamilies of MAPKs, high levels (0.1 μM) of activated murine p38α, rat JNK2, or rat ERK2 were used for in vitro phosphorylation of the GST-ELK1 substrate (Figure 4b). Reactions were carried out in the absence of RNA, in the presence of 0.12 μM family I or family II RNA, or at the same concentration of a random sequence pool of RNA (Figure 4b). Importantly, neither RNA family affected phosphorylation catalyzed by p38α or JNK2 (Figure 4b). In contrast, both family I and family II RNAs inhibited in vitro phosphorylation catalyzed by ppERK2 under these conditions, as expected given the K_i values for ppERK2 inhibition (Table 1). Random sequence RNA at this same concentration did not inhibit ppERK2-catalyzed phosphorylation (Figure 4b). Thus, RNAs belonging to both sequence families inhibit

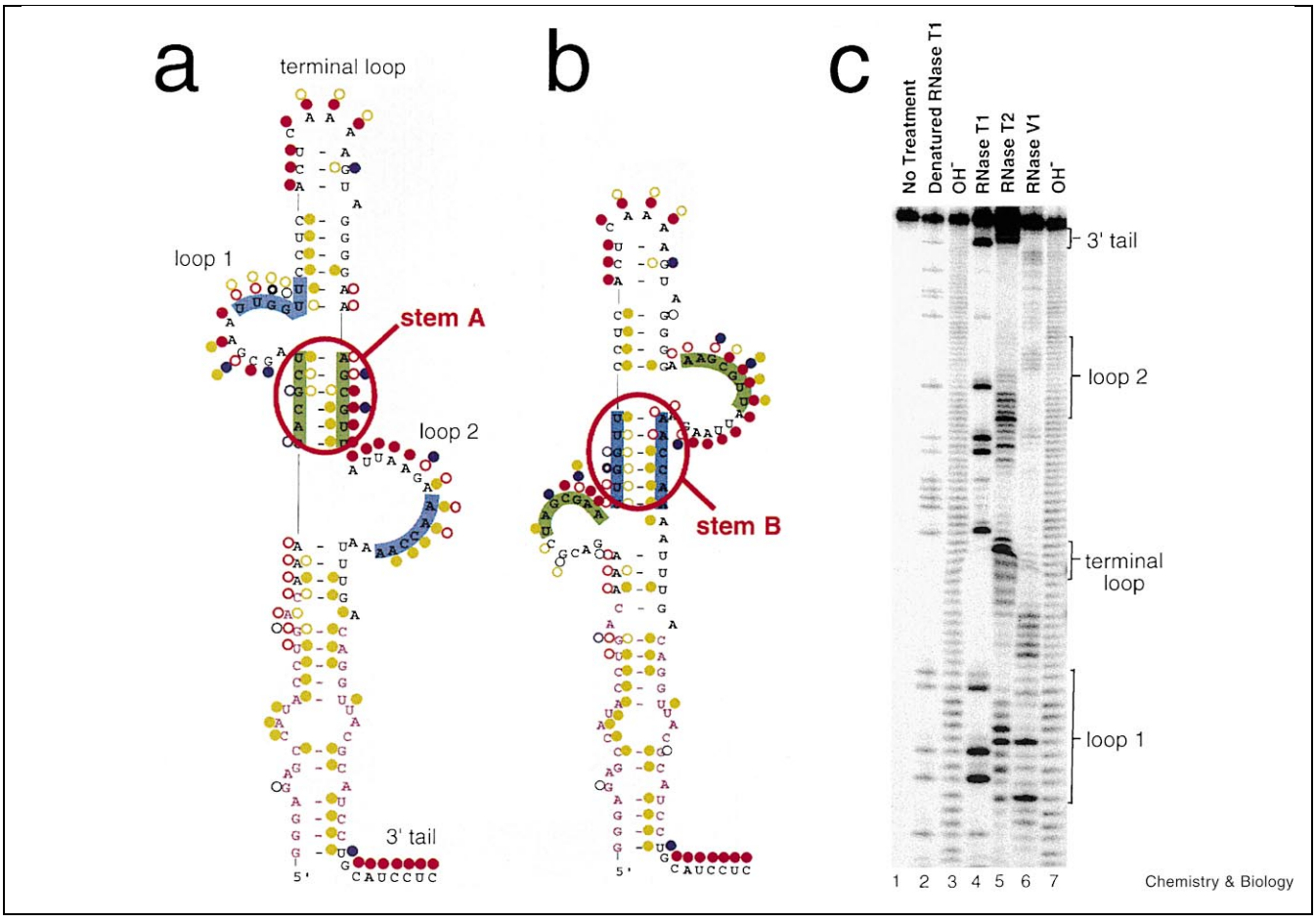

Figure 6. Analysis of the family II secondary structure. **(a)** Secondary structure model I. Mulford [23] predicted structure overlaid with summary results of nuclease structure probing experiments shown in panel **c**. Blue dots = RNase T1 sensitivity, red dots = RNase T2 sensitivity, yellow dots = RNase V1 sensitivity. For each nuclease, solid dots, partially filled dots, and open circles represent, respectively, strong, medium, and weak nuclease sensitivity. Sequences shown in purple are common to all library members. Sequences in loops 1 and 2 that are complementary are highlighted in blue. **(b)** Secondary structure model II. Alternate structure formed if internal loops in structure I instead form base pairs. **(c)** Structure probing by partial nuclease digestion. Digestions were performed under conditions in which family II Δ3′ inhibits ppERK2. Representative data are shown. 5′ end labeled family II Δ3′ RNA was partially digested with RNase T1 under denaturing conditions (lane 1), or hydrolyzed with alkali (lanes 2 and 7) as markers. Partial nuclease digestion of family II Δ3′ RNA with RNase T1 (lane 3), RNase T2 (lane 4), or RNase V1 (lane 6) was performed under conditions in which this RNA inhibits ppERK2 catalyzed phosphorylation. Terminal loop, 3′-tail, and internal loops 1 and 2 (see panel **a**) are indicated with brackets.

the two MAPKs (ERK1/2) that function in the signaling pathways mediating growth factor responses, but do not target MAPKs in cell stress or inflammatory signal transduction pathways.

Several lines of evidence support the conclusion that the family II inhibitor functions by interacting with the activation lip of ppERK1/2. First, family II preferentially associates with the phosphorylated form of ERK2 over the unphosphorylated form (Figure 2). Since conformational changes upon phosphorylation are largely localized to the activation lip and the P+1 specificity region of ERK2 (the majority of the kinase structure is static) [11], the binding preference for the phosphorylated form of the protein is consistent with RNA interaction with the activation lip. Second, family II blocks association of both the substrate and ATP (Figure 3, Table 1), which bind in close proximity to the activation lip [11]. Third, family II inhibits two different MAPKs with identical activation lip sequences (Figure 4a), but does not inhibit MAPKs with divergent sequences in this region (Figure 4b).

Family I associates with and inhibits ppERK at a lower concentration than does family II (Figure 2, Table 1, and data not shown), but functions in a different manner. In contrast to family II, family I does not recognize the acti-

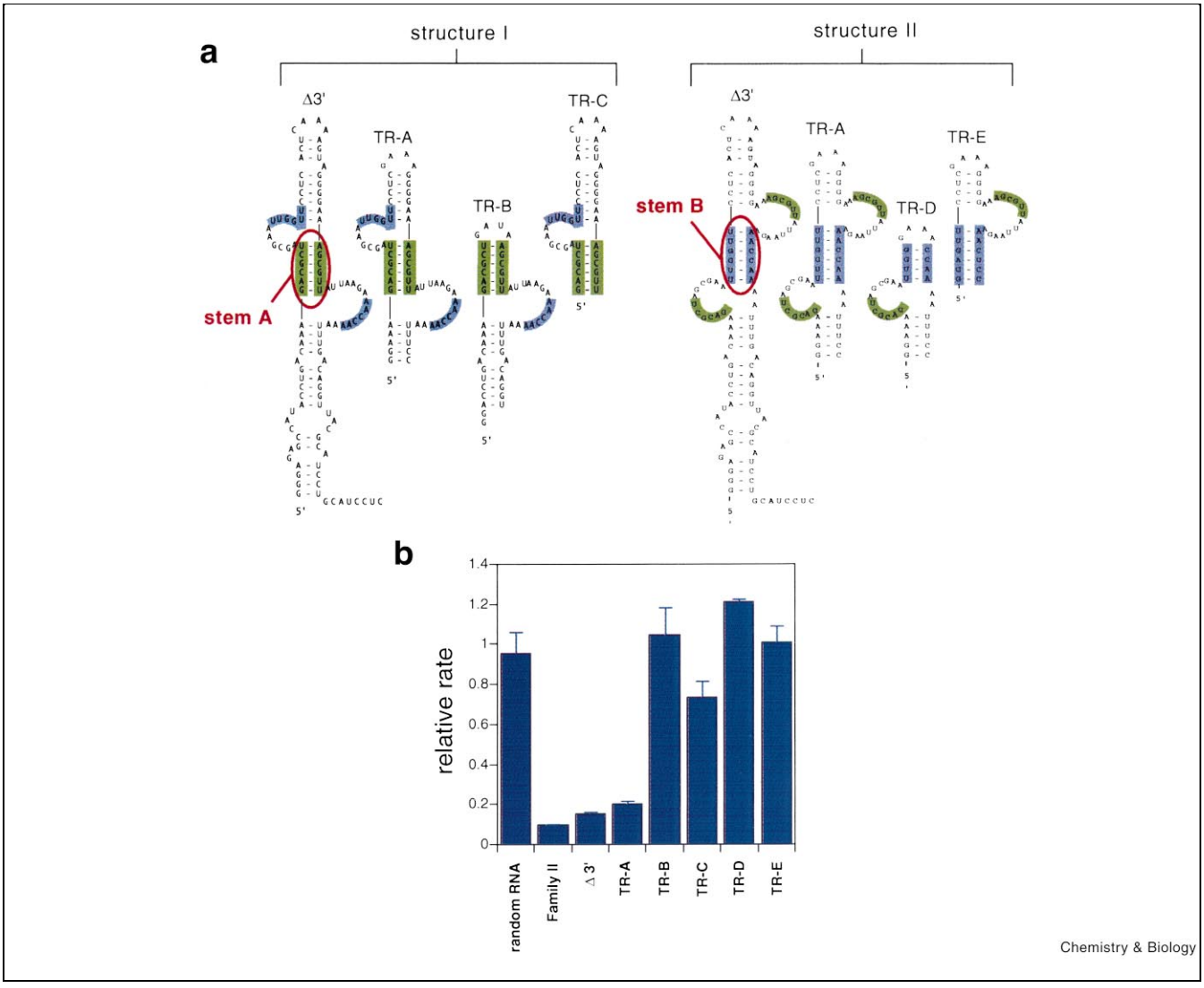

Figure 7. RNA truncations of the family II inhibitor. **(a)** Structural models of family II Δ3′ RNA. Alternative structural forms of the family II Δ3′ RNA are shown. The computer predicted structure, structure I, forms helix A (green). Structure II forms helix B (blue). RNA TR-A (truncation-A) can form both structures. RNA TR-B and RNA TR-C can form only the lower and upper portions of structure I, respectively, while RNA TR-D and RNA TR-E form the lower and upper portions, respectively, of structure II. **(b)** Inhibitory activity of truncated RNAs. All data are derived from two or more measurements, but in some cases errors are too small be visualized. In vitro phosphorylation reactions were carried out as in Figure 5, but contained the RNAs listed in panel **a**, the initial RNA pool, or no RNA.

vation lip since it associates with phosphorylated and unphosphorylated ERK2 with roughly the same affinity (see above). Thus, family I and family II inhibit ppERK2 by targeting different aspects of kinase structure.

RNA structural characterization

In an attempt to determine which part of family I and family II RNA was responsible for inhibition, truncated versions of each were tested for their ability to inhibit phosphorylation catalyzed by ppERK2 in vitro. As an initial means to localize inhibitory function, molecules containing only the 5′ half of the family I RNA or the family II RNA were tested for inhibitory activity (Figure 5). When ppERK2 was present at 10 nM, 20 nM of the family II RNA or 20 nM of an RNA representing its 5′-most 101 nucleotides (family II Δ3′) were equally effective at inhibiting ppERK2 function. In contrast, an RNA resulting from analogous truncation of family I RNA (family I Δ3′) did not display the complete inhibitory activity possessed by its parental RNA. No inhibitory activity was observed using RNAs corresponding to the 3′ half of either RNA family (data not shown). Thus, the family II RNA has a relatively

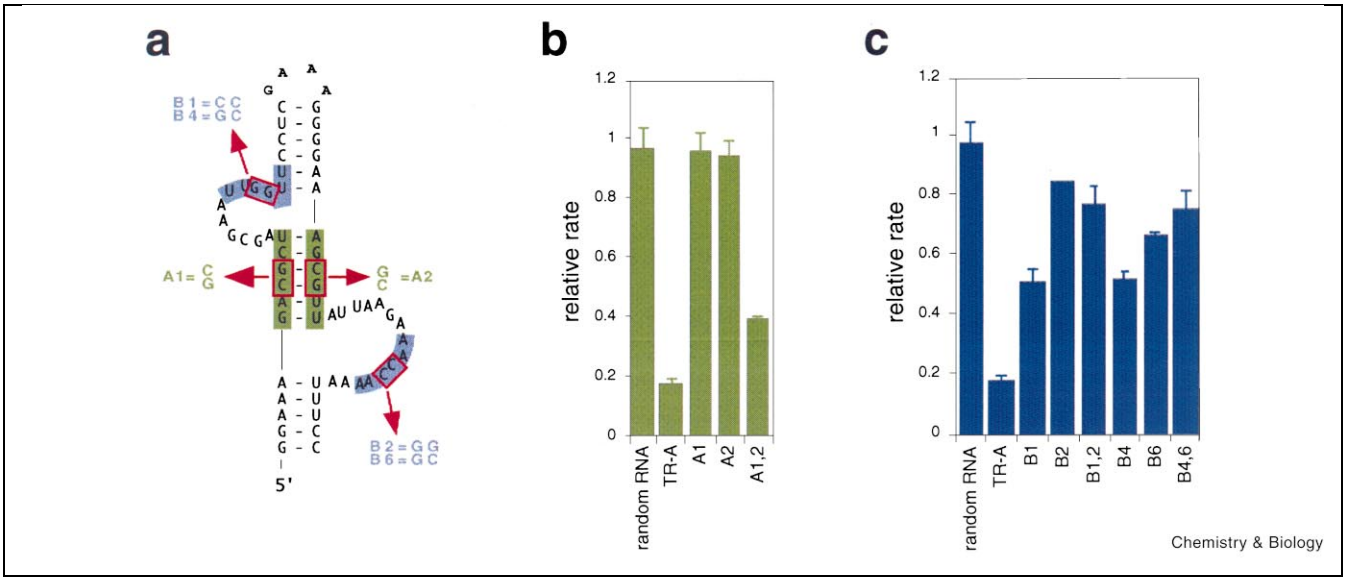

Figure 8. Mutants of family II inhibitor. **(a)** Secondary structural model and mutations. Structure I is shown and mutations in stem A and stem B are indicated as A series and B series mutations, respectively. **(b)** ppERK2 inhibition promoted by stem A mutants. All data are derived from two or more measurements, but in some cases errors are too small be visualized. Phosphorylation of 1.25 μM GST-ELK1 catalyzed by 10 nM ERK2 measured with 20 nM TR-A or 20 nM mutant RNA as indicated, or without RNA. The double mutant A1,2 restores stem A base pairing. Data are expressed as average relative rates, $k_{rel} = k_{RNA}/k_{no\ RNA}$, from two experiments. **(c)** ppERK2 inhibition promoted by stem B mutants. Same as in panel **b**, except the indicated RNAs were assayed. Double mutants that restore potential stem B base pairs are B1,2 and B4,6.

compact inhibitory region which is localized to its 5′-most 101 nucleotides, while the family I RNA has a less easily identifiable inhibitory region. Since family I does not bind to structural features particular to ppERK2 (e.g., the activation lip), it may require a larger portion of the RNA in order to promote a steric clash with protein substrate binding.

To investigate the family II RNA structural elements required for its inhibitory function, a computational model for the P22 Δ3′ RNA secondary structure was first generated ([23], structure I, Figure 6a). Family II Δ3′ RNA is predicted to consist of an extensive duplex with two large internal loops; a portion of this duplex is formed by sequences common to all library members. Interestingly, the two internal loops have regions that are complementary to one another. Thus, the P22 Δ3′ RNA could adopt an alternative structure in which the duplex between the internal loops (stem A, Figure 6a) is disrupted and a portion of the internal loops form an alternative duplex (stem B in structure II, Figure 6b).

To directly examine the solution structure of P22 Δ3′ RNA, it was subjected to partial digestion using nucleases with a preference for either single or double stranded RNA (Figure 6c). Regions of predicted duplex RNA common to both structures are sensitive to RNase V1, a nuclease specific for nucleotides that are in duplexes or that are stacked. The predicted terminal loop and the 3′-tail also common to both structures are sensitive to the single strand-specific nucleases RNase T1 and RNase T2. In support of structure I, the predicted internal loops of structure I are also sensitive to RNase T1 and RNase T2 (Figure 6a). However, several nucleotide positions in these loops are also sensitive to RNase V1. These same positions form helix B in structure II (Figure 6b). Similarly, sequences comprising stem A in structure I and stem B in structure II are sensitive to both single and double strand-specific nucleases (Figure 6a,b). Since our RNA selection methodology did not require conformational homogeneity of functional RNAs, our interpretation of these data is that both structures exist in equilibrium in solution.

To determine which one of these two structures inhibited ppERK2, additional truncations of the family II Δ3′ RNA were made to further localize the ppERK2 inhibitory domain. A mutant RNA that replaced the terminal loop and three putative base pairs adjacent to it with a tetraloop and also removed sequences common to all library members was first constructed (RNA TR-A, Figure 7a). TR-A is still capable of forming both of the alternative helices (stems A and B) present in structure I and structure II, respectively. This RNA inhibited ppERK2 activity in a manner nearly identical to the family II Δ3′ and the full length family II

RNA (Figure 7b). More drastic truncations were made in an attempt to associate ppERK2 inhibition with one of the two alternative structures. However, RNAs representing the lower or the upper portions of structure I (RNAs TR-B and TR-C, respectively, Figure 7a) or the lower or upper half of structure II (TR-D and TR-E, Figure 7a) all failed to inhibit ppERK2 (Figure 7b). Thus, many of the sequence and/or structural elements within TR-A are essential for inhibitory activity.

To examine directly the importance of stems A and B for ppERK2 inhibitory activity, mutations that disrupted each stem were introduced into TR-A (Figure 8a). Disruption of putative stem A by changing the sequence of either strand (mutations A1 and A2, Figure 8a) resulted in a complete loss of inhibitory function (Figure 8b). Restoration of potential base pairing in stem A upon combining these two mutations (A1,2) resulted in an RNA that possessed inhibitory activity, albeit slightly reduced (Figure 8b). Thus, stem A is a required structural component of the family II RNA but its particular sequence is not. In contrast, mutations based upon structure II that disrupt putative stem B (B1, B2, B4 and B6) reduced, but did not completely eliminate, ppERK2 inhibition (Figure 8c). Mutations in the 5′ portion of the putative stem (B1 and B4) affected inhibitory activity the least (each displaying a $k_{rel} = 0.51$), while mutations in the 3′ portion (B2 and B6) had the greatest impact ($k_{rel} = 0.84$ and 0.66 for B2 and B6, respectively). Thus, the identities of these sequences are of differing importance, but both are nevertheless nonessential determinants of ppERK2 inhibition. Double mutants that restored the potential for stem B base pairing (B1,2; B4,6) failed to restore further ppERK2 inhibition (Figure 8b), suggesting that stem B is not a structural element required for ppERK2 inhibition. The sum of these mutagenesis data suggest that structure I is the functional motif. However, we cannot exclude the possible formation of a pseudoknotted RNA structure [24] in which both stems A and B form simultaneously since such a structure may require a specific nucleotide sequence in putative stem B [25].

Significance

All mitogenic stimuli are thought to activate the evolutionarily conserved RAS-RAF-MKK1/2-ERK1/2 pathway, and oncogenic alleles of RAS are found in greater than 50% of all colon carcinomas [2]. Despite a detailed understanding of the MAPK signal transduction cascade, the global changes in gene expression promoted by ERK1/2 that result in proliferative responses remain unknown. Specific inhibitors of ERK1/2 in conjunction with genome-wide expression profiling techniques would be invaluable tools to address such issues. Here, we report the in vitro characterization of RNA inhibitors of ppERK1/2, the first inhibitors developed that display specificity for these two kinases. The ppERK1/2 inhibitors described here will be useful tools in probing the functions of growth factor regulated MAPK pathways in vivo.

The approach we have used to develop ppERK1/2 inhibitors is readily generalizable and can be used to develop inhibitors of any chosen kinase provided it is expressed and purified. These RNA inhibitors function by a unique mechanism, distinct from that of small molecule protein kinase inhibitors, which involves the steric exclusion of substrate binding. Because these novel inhibitors interact with less conserved structural aspects of their target kinase, they could possess a much greater potential for specificity than small molecule inhibitors of ATP binding.

Materials and methods

Protein production and purification

$(His)_6$-tagged rat ERK2, human ERK1, and constitutively active human MKK1 (G7B: ΔN4/S218D/S222D [27]) were separately expressed in *Escherichia coli* BL21(DE3), pLYS-S and purified by nickel NTA-agarose affinity chromotography as previously described [26,27]. In vitro activation of ERK1 and ERK2 by MKK1-G7B was performed as reported [28]. Activated murine p38α and activated rat JNK2 were produced in vivo by coexpression with MEK4 and MEKK1C [29]. Myelin basic protein (MBP) was purchased (Sigma) and the glutathione *S*-transferase/ELK1 fusion protein (GST-ELK1 (307–428)) was expressed and purified as described [30].

Library construction and RNA iterative selection

The initial RNA pool was produced by in vitro transcription of a DNA library constructed as described [21]. This library had the general sequence 5′-AGCGAATTCTAATACGACTCACTATA//GGGAGAGCCATA-CCTGAC-N_{68}-CAGGTTACGCATCC-N_{66}-GTCAGTCGTCAGGATCCG-TG-3′, where N is a randomized nucleotide position and // represents the T7 RNA polymerase transcriptional start site. Approximately 2×10^{14} members of this library (44 μg) were transcribed with T7 RNA polymerase. In the first selection cycle, approximately 82 μg of the RNA pool (representing four copies of each RNA) was denatured in water at 90°C for 3 min and allowed to fold by slow cooling from 55°C to 30°C in 10 mM HEPES, pH 7.5, 10 mM $MgCl_2$. After folding, the pool RNA was passed through a nitrocellulose filter (HAWP, Millipore Inc.) and the filtrate was incubated at a concentration of 2.5 μM with 0.2 μM ppERK2 for 1 h at 30°C. RNA–protein complexes were collected by passing this solution through another HAWP filter. Bound RNA was released from the filter with 4 M guanidine thiocyanate, ethanol precipitated, and amplified by reverse transcription and PCR. After the fifth selection cycle, a negative selection step was introduced to remove pool RNAs also retained on HAWP filters in the presence of unphosphorylated ERK2. Four to six successive incubations and HAWP filtrations were used in each negative selection cycle. RNA and protein concentrations were each progressively dropped to 1 nM in a total of 15 subsequent selection cycles. cDNA derived from the last selection cycle was digested with *Eco*RI and *Hin*dIII and subcloned into similarly digested pUC19. Family I and family II RNA sequences were deposited in GenBank (accession numbers AF301132 and AF301133, respectively). Dissociation constants were determined as described [31].

Activity assays and kinetic analysis

MAPK catalyzed in vitro phosphorylation reactions were monitored by ^{32}P incorporation into either MBP or GST/ELK1 under conditions previously described [27]. Enzyme, substrate, and RNA inhibitor concentrations varied with experiment as indicated. Relative rates (k_{rel}) were calculated by dividing k_{obs} values obtained in the presence of RNA by a

k_{obs} value obtained in the absence of RNA but under otherwise identical conditions.

RNA mutants and nuclease structure probing

Truncated RNAs were produced by a variety of approaches. Family I Δ3′ and family II Δ3′ were obtained by run off transcription of pUC/family I and pUC/family II, respectively, following their digestion with *Sfa*NI, an enzyme whose recognition site was designed into the central constant region of the initial library. All other truncated RNA and mutant RNA variants were transcribed with T7 RNA polymerase after their construction. TR-A was produced by polymerase extension of the overlapping deoxyoligonucleotides TR-A/5′, 5′-AgC gAA TTC TAA TAC gAC TCA CTA TAg gAA AgA CgC TAg CgA ATT ggT TCC TCg AAA gg and TR-A/3′, 5′-ggA AAT TTT ggT TTC TTA ATA ACg CTT TCC CCT TTC gAg gAA CCA ATT Cg. DNAs encoding A.1; A.2; A.1,2; B.1; B.2; B.1,2; B.3; B.5; B.3,5; B.4; B.6 and B.4,6 were similarly produced, but deoxyoligonucleotides carried the mutations indicated in Figure 8a. TR-D and TR-E were produced by Milligan transcription [32] of deoxyoligonucleotides 5′-GGA GTT TCT TAA TAA CGC TTT CCC CTT TCG AGG AAC TCC TAT AGT GAG TCG TAT TAG AAT TCG CT and 5′-GGA AAT TTT GGT TTC CCA ATT CGC TAG CGT CTT TCC TAT AGT GAG TCG TAT TAG AAT TCG CT, respectively. TR-B was produced by priming PCR of full length family II DNA with deoxyoligonucleotides 5′-AgC gAA TTC TAA TAC gAC TCA CTA TAg ggA CgC TAg CgA ATT gg and 5′-AAC gCT TTC CCC TAC. TR-C was produced by polymerase extension of the overlapping deoxyoligonucleotides 5′-AgC gAA TTC TAA TAC gAC TCA CTA TAg gAC CTg ACA AAg Acg CTg ATA AgC g and 5′-ACC TgT CAA ATT TTg gTT TCT TAA TAA CGc TTA TcA Gcg Tc.

Computer predictions of RNA secondary structure were made using Mulfold [23] running on an Apple G3 Powerbook. Prior to nuclease structure probing experiments the concentration of RNase T1 (Sigma Chemical Corp.), RNase T2 (CalBiochem, Inc.) and RNase V1 (Amersham/Pharmacia Biotech Inc.) required for partial RNA digestion was empirically determined.

Acknowledgements

We thank Melanie Cobb (University of Texas, Southwestern) for ERK1, ERK2, active p38 and active JNK expression constructs; Kun-Liang Guan (University of Michigan) for the GST-ELK1 expression construct; and Kevin Polach for comments on the manuscript. This work was supported by Grants NIH AI-30242 and GM48521 to O.C.U. and N.G.A., respectively. S.D.S. was supported by a Helen Hay Whitney Postdoctoral fellowship.

References

1. Lewis, T.S., Shapiro, P.S. & Ahn, N.G. (1998). Signal transduction through MAP kinase cascades. *Adv. Cancer Res.* **74**, 49–139.
2. Hanahan, D. & Weinberg, R.A. (2000). The hallmarks of cancer. *Cell* **100**, 57–70.
3. Lewis, A.J. & Manning, A.M. (1999). New targets for anti-inflammatory drugs. *Curr. Opin. Chem. Biol.* **3**, 489–494.
4. Kültz, D. (1998). Phylogenetic and functional classification of mitogen- and stress-activated protein kinases. *J. Mol. Evol.* **46**, 571–588.
5. Tong, L., Pav, S., White, D.M., Rogers, S., Crane, K.M., Cywin, C.L., Brown, M.L. & Pargellis, C.A. (1997). A highly specific inhibitor of human p38 MAP kinase binds in the ATP pocket. *Nature Struct. Biol.* **4**, 311–316.
6. Young, P.R., McLaughlin, M.M., Kumar, S., Kassis, S., Doyle, M.L., McNulty, D., Gallagher, T.F., Fisher, S., McDonnell, P.C., Carr, S.A., Huddleston, M.J., Seibel, G., Porter, T.G., Livi, G.P., Adams, J.L. & Lee, J.C. (1997). Pyridinyl imidazole inhibitors of p38 mitogen-activated protein kinase bind in the ATP site. *J. Biol. Chem.* **272**, 12116–12121.
7. Kovalenko, M., Ronnstrand, L., Heldin, C.H., Loubtchenkov, M., Gazit, A., Levitzki, A. & Bohmer, F.D. (1997). Phosphorylation site-specific inhibition of platelet-derived growth factor beta-receptor autophosphorylation by the receptor blocking tyrphostin AG1296. *Biochemistry* **36**, 6260–6269.
8. Traxler, P.M., Furet, P., Mett, H., Buchdunger, E., Meyer, T. & Lydon, N. (1996). 4-(Phenylamino)pyrrolopyrimidines: potent and selective, ATP site directed inhibitors of the EGF-receptor protein tyrosine kinase. *J. Med. Chem.* **39**, 2285–2292.
9. Salituro, F.G., Germann, U.A., Wilson, K.P., Bemis, G.W., Fox, T. & Su, M.S. (1999). Inhibitors of p38 MAP kinase: therapeutic intervention in cytokine-mediated diseases. *Curr. Med. Chem.* **6**, 807–823.
10. Eyers, P.A., Craxton, M., Morrice, N., Cohen, P. & Goedert, M. (1998). Conversion of SB 203580-insensitive MAP kinase family members to drug-sensitive forms by a single amino-acid substitution. *Chem. Biol.* **5**, 321–328.
11. Canagarajah, B.J., Khokhlatchev, A., Cobb, M.H. & Goldsmith, E.J. (1997). Activation mechanism of the MAP kinase ERK2 by dual phosphorylation. *Cell* **90**, 859–869.
12. Gold, L., Polisky, B., Uhlenbeck, O. & Yarus, M. (1995). Diversity of oligonucleotide functions. *Annu. Rev. Biochem.* **64**, 763–797.
13. Gal, S.W., Amontov, S., Urvil, P.T., Vishnuvardhan, D., Nishikawa, F., Kumar, P.K. & Nishikawa, S. (1998). Selection of a RNA aptamer that binds to human activated protein C and inhibits its protease function. *Eur. J. Biochem.* **252**, 553–562.
14. Bell, S.D., Denu, J.M., Dixon, J.E. & Ellington, A.D. (1998). RNA molecules that bind to and inhibit the active site of a tyrosine phosphatase. *J. Biol. Chem.* **273**, 14309–14314.
15. Conrad, R., Keranen, L.M., Ellington, A.D. & Newton, A.C. (1994). Isozyme-specific inhibition of protein kinase C by RNA aptamers. *J. Biol. Chem.* **269**, 32051–32054.
16. Bertrand, E., Castanotto, D., Zhou, C., Carbonnelle, C., Lee, N.S., Good, P., Chatterjee, S., Grange, T., Pictet, R., Kohn, D., Engelke, D. & Rossi, J.J. (1997). The expression cassette determines the functional activity of ribozymes in mammalian cells by controlling their intracellular localization. *RNA* **3**, 75–88.
17. Ilves, H., Barske, C., Junker, U., Bohnlein, E. & Veres, G. (1996). Retroviral vectors designed for targeted expression of RNA polymerase III-driven transcripts: a comparative study. *Gene* **171**, 203–208.
18. Blind, M., Kolanus, W. & Famulok, M. (1999). Cytoplasmic RNA modulators of an inside-out signal-transduction cascade. *Proc. Natl. Acad. Sci. USA* **96**, 3606–3610.
19. Thomas, M., Chedin, S., Carles, C., Riva, M., Famulok, M. & Sentenac, A. (1997). Selective targeting and inhibition of yeast RNA polymerase II by RNA aptamers. *J. Biol. Chem.* **272**, 27980–27986.
20. Shi, H., Hoffman, B.E. & Lis, J.T. (1999). RNA aptamers as effective protein antagonists in a multicellular organism. *Proc. Natl. Acad. Sci. USA* **96**, 10033–10038.
21. Zhang, B. & Cech, T.R. (1997). Peptide bond formation by in vitro selected ribozymes. *Nature* **390**, 96–100.
22. Frantz, B., Klatt, T., Pang, M., Parsons, J., Rolando, A., Williams, H., Tocci, M.J., O'Keefe, S.J. & O'Neill, E.A. (1998). The activation state of p38 mitogen-activated protein kinase determines the efficiency of ATP competition for pyridinylimidazole inhibitor binding. *Biochemistry* **37**, 13846–13853.
23. Zuker, M., Mathews, D.H. & Turner, D.H. (1999). Algorithms and thermodynamics for RNA secondary structure prediction: A practical guide. In *RNA Biochemistry and Biotechnology*. (Barciszewski, J. and Clark, B.F.C., eds.), pp. 11–43, Kluwer Academic, Dordrecht.
24. Puglisi, J.D., Wyatt, J.R. & Tinoco, I.J. (1988). A pseudoknotted RNA oligonucleotide. *Nature* **331**, 283–286.
25. Su, L., Chen, L., Egli, M., Berger, J.M. & Rich, A. (1999). Minor groove RNA triplex in the crystal structure of a ribosomal frameshifting viral pseudoknot. *Nature Struct. Biol.* **6**, 285–292.
26. Robbins, D.J., Zhen, E., Owaki, H., Vanderbilt, C.A., Ebert, D., Geppert, T.D. & Cobb, M.H. (1993). Regulation and properties of extracellular signal-regulated protein kinases 1 and 2 in vitro. *J. Biol. Chem.* **268**, 5097–5106.
27. Mansour, S.J., Candia, J.M., Matsuura, J.E., Manning, M.C. & Ahn, N.G. (1996). Interdependent domains controlling the enzymatic activity of mitogen-activated protein kinase kinase 1. *Biochemistry* **35**, 15529–15536.

28. Shapiro, P.S., Vaisberg, E., Hunt, A.J., Tolwinski, N.S., Whalen, A.M., McIntosh, J.R. & Ahn, N.G. (1998). Activation of the MKK/ERK pathway during somatic cell mitosis: direct interactions of active ERK with kinetochores and regulation of the mitotic 3F3/2 phosphoantigen. *J. Cell Biol.* **142**, 1533–1545.
29. Khokhlatchev, A., Xu, S., English, J., Wu, P., Schaefer, E. & Cobb, M.H. (1997). Reconstitution of mitogen-activated protein kinase phosphorylation cascades in bacteria. Efficient synthesis of active protein kinases. *J. Biol. Chem.* **272**, 11057–11062.
30. Marais, R., Wynne, J. & Treisman, R. (1993). The SRF accessory protein Elk-1 contains a growth factor-regulated transcriptional activation domain. *Cell* **73**, 381–393.
31. Dertinger, D., Behlen, L.S. & Uhlenbeck, O.C. (2000). Using phosphorothioate-substituted RNA to investigate the thermodynamic role of phosphates in a sequence specific RNA-protein complex. *Biochemistry* **39**, 55–63.
32. Milligan, J.F. & Uhlenbeck, O.C. (1989). Synthesis of small RNAs using T7 RNA polymerase. *Methods Enzymol.* **180**, 51–62.